L.3

LAMS-2488

LOS ALAMOS SCIENTIFIC LABORATORY

OF THE UNIVERSITY OF CALIFORNIA o LOS ALAMOS NEW MEXICO

QUARTERLY STATUS REPORT OF THE LASL CONTROLLED THERMONUCLEAR RESEARCH PROGRAM FOR PERIOD ENDING NOVEMBER 20, 1960

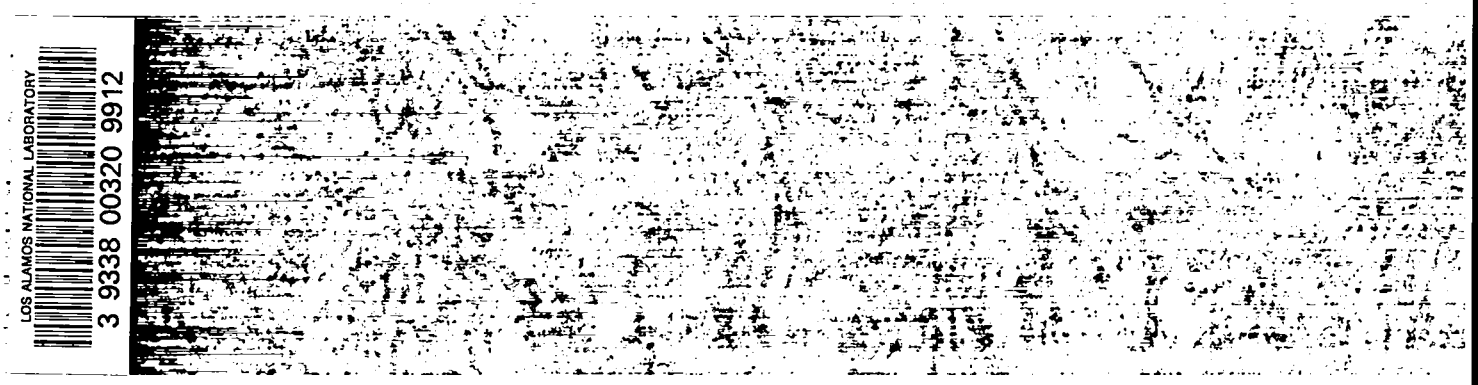

Printed in USA. Price $1.00. Available from the

Office of Technical Services
U. S. Department of Commerce
Washington 25, D. C.

LAMS-2488
CONTROLLED THERMONUCLEAR
PROCESSES
TID-4500, 15th Ed.

LOS ALAMOS SCIENTIFIC LABORATORY
OF THE UNIVERSITY OF CALIFORNIA LOS ALAMOS NEW MEXICO

REPORT COMPILED: December 1960
REPORT DISTRIBUTED: December 30, 1960

QUARTERLY STATUS REPORT OF THE LASL CONTROLLED THERMONUCLEAR RESEARCH PROGRAM FOR PERIOD ENDING NOVEMBER 20, 1960

Prepared from material supplied by P Division

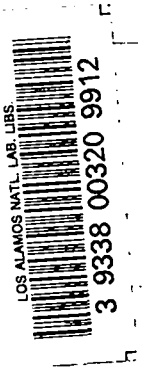

Contract W-7405-ENG. 36 with the U. S. Atomic Energy Commission

SHERWOOD PROGRAM QUARTERLY REPORT

SUMMARY

1. In the entropy trapping experiment measurements have been made of the energy of the ions escaping through the ring cusp of the picket fence magnet. Ion energies from 50 ev to 3 kev have been observed, the 50 ev particles lasting ~ 20 μsec and the 3 kev particles disappearing ~ 3 μsec after plasma injection. Indications are that these particles are not from the trapped high-β region in the central volume of the magnet but are rather single particles which are directed from the gun along magnetic field lines out of the ring cusp. The design of a large caulked picket fence machine (vacuum vessel 150 cm diameter, 300 cm long) has been completed and delivery is expected in February, 1961. Meanwhile a half-scale model has been assembled to determine scaling laws.

2. The search for a contained beam of injected 7.0-kev protons in the skew trapping experiment has continued for the symmetric magnet configuration. When the beam is injected ~ 2.5 cm off axis and inclined 5° to the plane of the axis, a detector located in the ring cusp exhibits a persistent tail ~ 100 μsec long after the beam has been pulsed off. It is not known whether this signal represents an ion beam contained for these times or is due to (a) perturbations in the injector from stray magnetic fields, or (b) residual electrons in the containment volume striking the detector.

3. The first phase of the diagnostic program on the behavior of the plasma in a coaxial gun has been completed. A qualitative picture of the gun's performance has been obtained.

4. Measurements on the yield of D-D neutrons from Perhapsatron S-5 Zeus show dependences on the B_z stabilizing magnetic field, applied voltage, and gas pressure similar to those observed earlier with the smaller machines. Impurity radiation (3500 to 8000 A) consisting of a strong continuum with broadened line spectra (predominantly silicon and oxygen) is observed with an onset time near peak gas current (~ 30 μsec after initiation of the gas discharge).

5. The electron density in the microwave scattering experiment has been increased by a factor of 50 to a value of about 10^{10} electrons/cm^3 by the addition of small quantities of krypton and mercury. The radiation pattern produced by the primary power S-band horn has been examined and it is estimated that the intensity of the primary beam inside the bottle is approximately 1/40 watt/cm^2.

6. Kerr cell photographs have been taken of the discharge in the orthogonal pinch experiment. The photographs show weak diffuse regions of light which have some boundary irregularities during the second half-cycle. No sharply defined boundaries exist as reported from other experiments. X-ray photographs made with a pinhole camera through a thin (~ 225 μg/cm^2) aluminum-Zapon window give images which indicate a region of hot electrons ($0.1 < T_e < 0.5$ kev) of diameter 1.2 to 2.0 cm.

7. The striking conclusion has been reached that the energy loss in Ixion, leading to the voltage-limiting effect, which arises from current drawn across the device, resides predominantly in hard ultraviolet radiation from impurity ions, much as in the case of the toroidal pinch Perhapsatron S-4. A major portion of the Ixion plasma is fully ionized; hence, ion-neutral and electron-neutral collisions need not be invoked to account for the voltage limiting process. There is now reason to believe that the ion energy may be raised to the kev region if a clean system is constructed.

A new plasma accelerator - the E X B gun - is being constructed in place of the old Ixion.

8. Construction of Scylla III is complete. After delays occasioned by electrical and mechanical difficulties, the machine has been fired, using second half-cycle operation. The neutron yield has increased by an order of magnitude. Work on a preionizer is proceeding.

Scylla I's x-rays have been successfully diffracted with the beryl crystal soft x-ray spectrometer. Previously unobserved Lyman and helium-like, singlet and triplet series lines are observed in the spectra of O VIII, Ne IX, and Ne X when these elements are introduced into the gas of the discharge.

9. Installation of the first half of the Zeus capacitor bank has essentially been completed and preparations are underway for testing the newly installed sections. Work is proceeding on the conversion of one tier of the bank to a faster (low-inductance) transmission system.

10. In order to determine the relative merits of various energy storage capacitors now available, an extensive program is under way to measure the capacity, Q value,and ringing frequency of all units in use at LASL as well as several others of new types.

11. Development work has been proceeding on a fast parallel plate capacitor; two prototype units have been constructed and are being evaluated.

A. ENTROPY TRAPPING

Measurements of ions escaping from the ring cusp of the picket fence magnet have been made using a collimated magnetic momentum analyzer followed by a post-acceleration section and a detector with an aluminum coated plastic scintillator-photomulitplier combination. Particles from 50 ev to 3 kev have been observed escaping, the 50 ev particles lasting $\sim$ 20 μsec and the 3 kev particles disappearing in $\sim$ 3 μsec after plasma injection into the picket fence. Indications are that these particles escaping through the ring cusp are not from the trapped high-β region, but rather they are tied to individual field lines outside this region. The time duration of the escaping particles appears to be due to multiple reflections at the cusps and the associated time spread resulting from the velocity dispersion of the particles (input time duration of 2 to 5 μsec at the input cusp). The fate of the particles producing the trapped $\beta \sim 1$ region is not understood, but they may be lost simply by diffusion across the magnetic fields if the electron temperature is too low (less than 10 ev).

The design of the large caulked picket fence (vacuum vessel 60 in. diam and 120 in. long) has been completed and the apparatus should be received about February 1, 1961. A smaller (half scale) version of this system has been built to test the concept of the caulked picket fence and to determine scaling laws. The apparatus is temporary but some experimental work can be done with it before completion of the full-scale equipment. A rearrangement of the experimental area has taken 2 months; however, the new floor plan gives this experimental group enough room so that two cusped field experiments may be set up at the same time and also provides an area for gun study.

B. PLASMA GUN DIAGNOSTICS

The first phase of the diagnostic program on behavior of the plasma in a coaxial accelerator has been completed. For a given set of operating parameters, the following qualitative picture of the gun's performance was obtained:

1) The current flows initially in a thin radial current sheet which forms approximately over the gas inlet ports in the center conductor (cathode). This sheet, for a voltage of 16 kv on the 15 μfd storage capacitor, and 3×10^{-5} g injected deuterium, accelerates to a velocity of 1.5×10^{7} cm/sec in 10 cm. The sheet always remains flat and perpendicular to the axis. A plot of position vs time is given in Fig. 1.

2) As it moves down the barrel, the current layer develops a "tail," i.e., part of the total radial current begins to flow over a considerable depth behind the front. The fraction of the total current carried by the sheet decreases steadily until it disappears entirely, leaving only the broad tail. This sequence of events is seen in Fig. 2, where the slope of the B_θ distribution, i.e., $\partial B_\theta / \partial z$, is proportional to radial current density.

3) Measurements with electric probes indicate that there is a voltage drop of about 200 volts near the cathode as shown in Fig. 3. This suggests that the phenomena occurring here may be similar to those found in a glow discharge rather than an arc.

4) The thin current sheet does not retain all the gas it encounters. A calculation, using the measured velocity history and magnetic driving pressure, showed that after it had moved 5 cm, the sheet accumulated no net mass, whereas perfect snowplow action would have subsequently doubled its mass. Figure 4 shows the velocity of the sheet, together with the velocity obtained by assuming no mass increase after 0.9 μs.

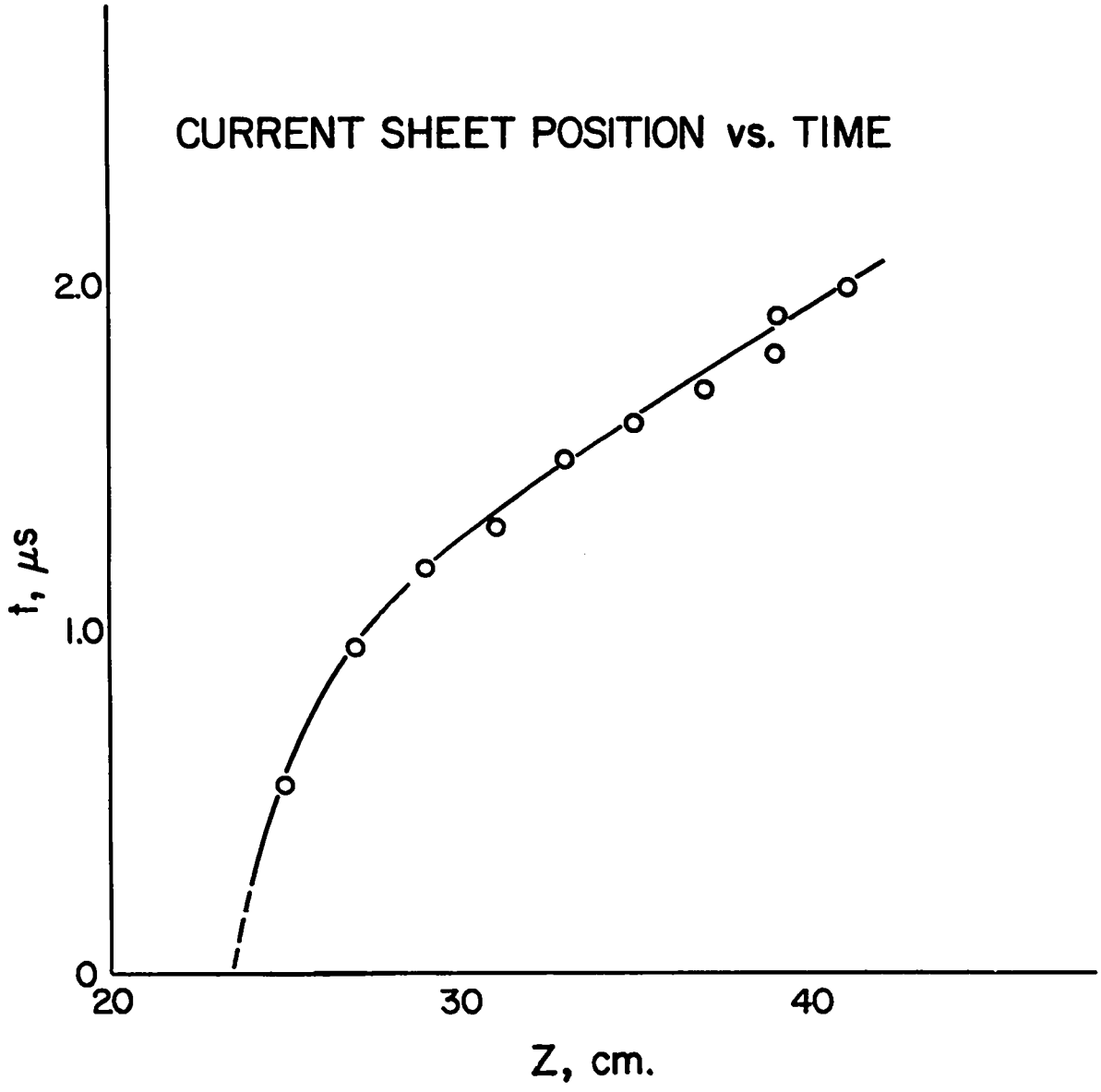

Fig. 1. Current sheet position in plasma gun versus time.

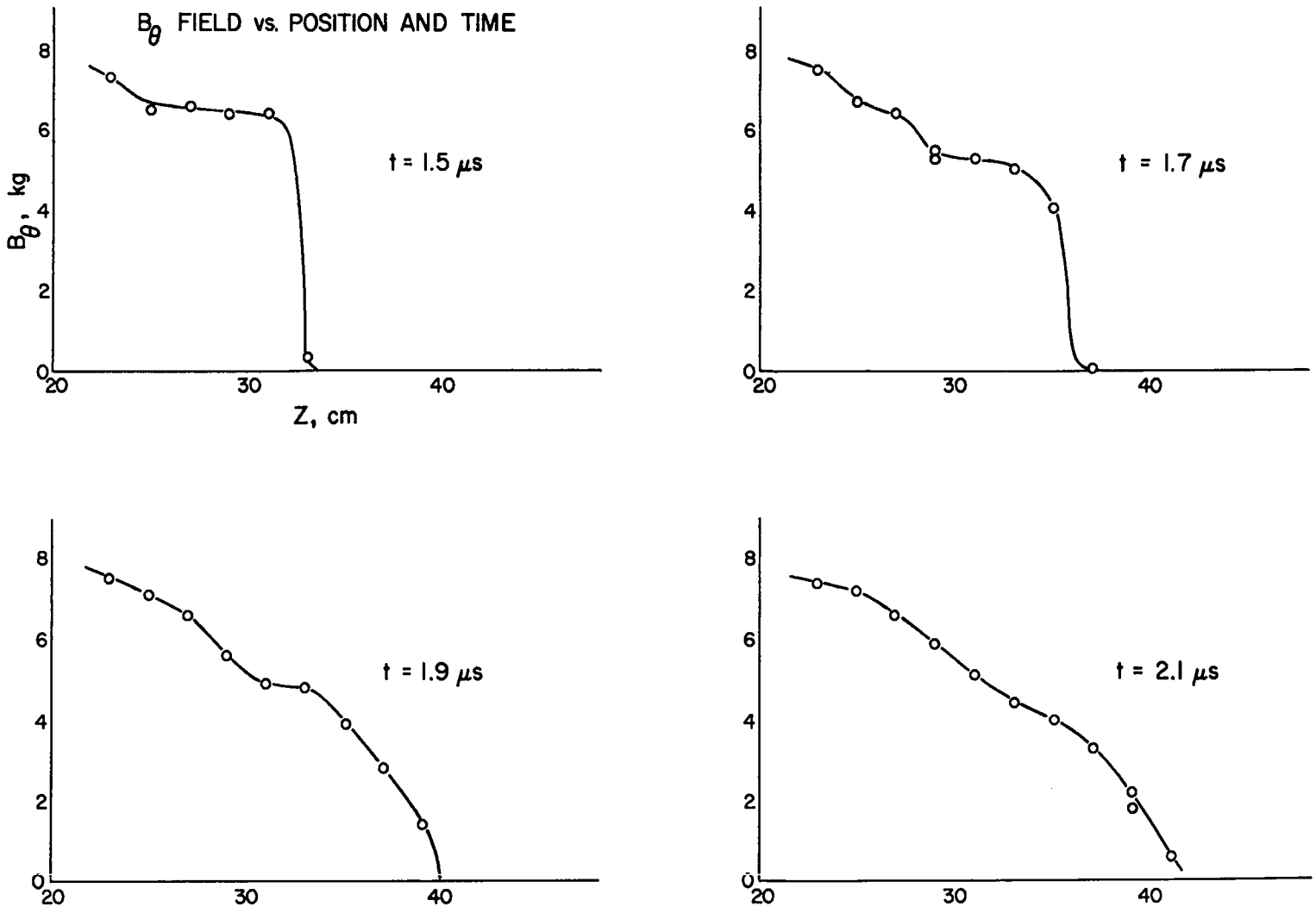

Fig. 2. B_θ-field in plasma gun versus position and time.

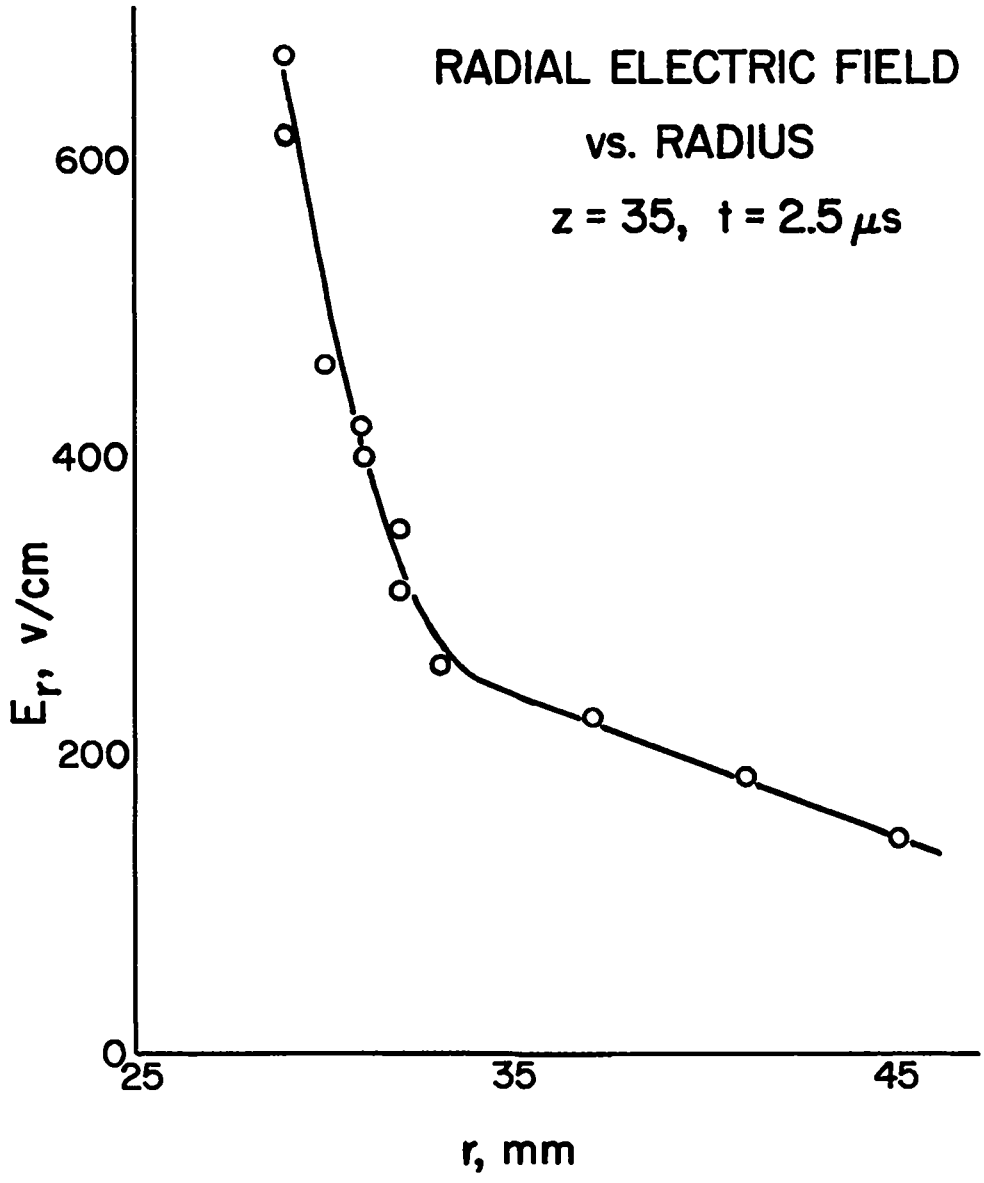

Fig. 3. Radial electric field in plasma gun versus radius

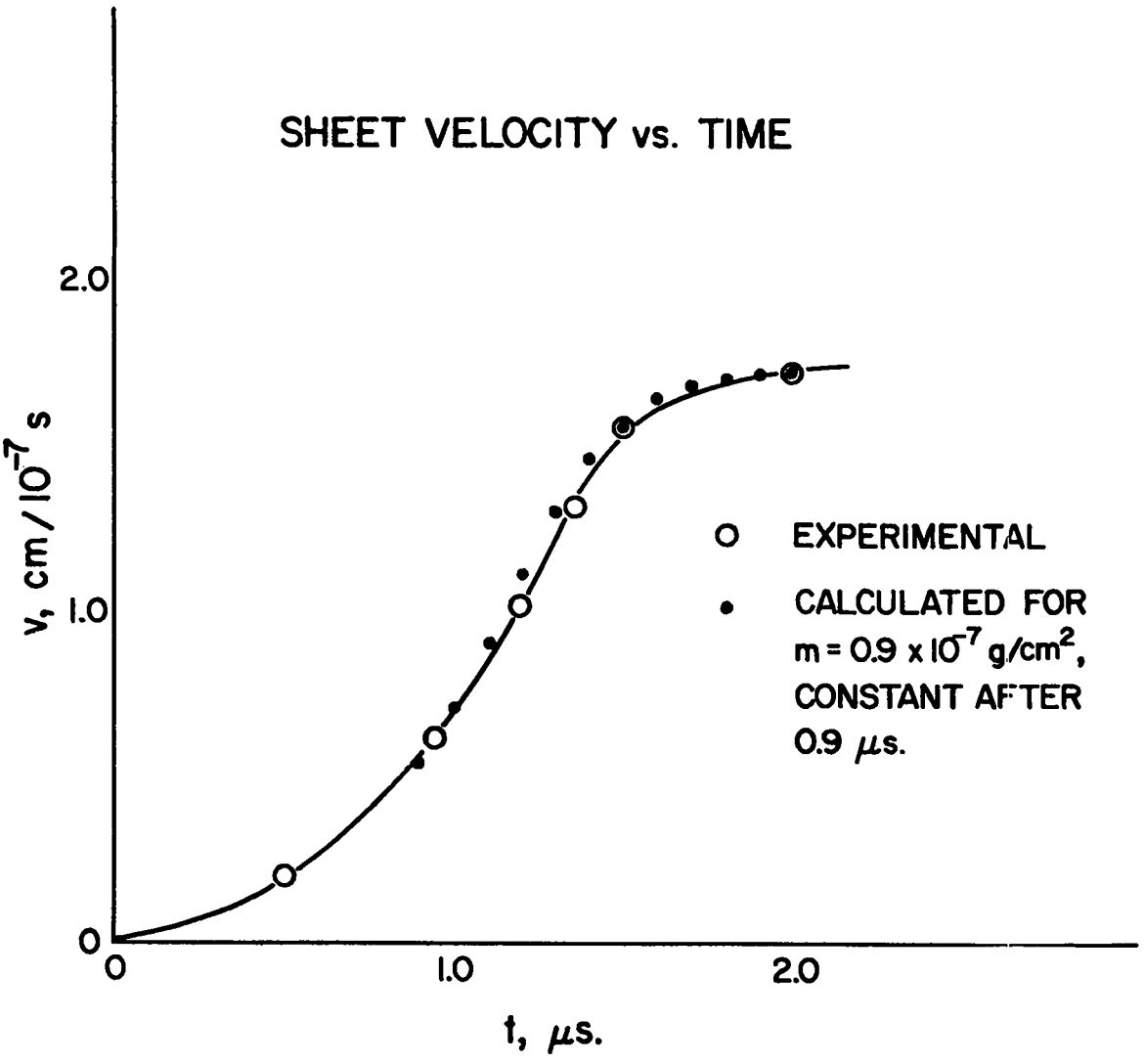

Fig. 4. Sheet velocity in plasma gun versus time.

The reason for the flatness of the current sheet is obscure, since the magnetic pressure behind that part nearest the cathode is nearly four times that near the anode. It is possible that the current sheet is some special variety of shock wave. The failure of the front to increase its mass is not readily explained, but it appears, from a simple calculation, that the ionization probability for a deuterium molecule overtaken by the current sheet drops rapidly below unity as the plasma temperature goes below 10 ev, a probable value for the gun.

C. SKEW TRAPPING

The energy of the ion gun used for injection into the skew trapping magnet has been lowered to 7 kev. This has eliminated the loss due to particles striking the vacuum chamber at the corners protruding into the magnetic field near the line cusp, as previously reported (LAMS-2464, p. 11). With this 7-kev beam, the experiments demonstrating reflection from the back point cusp were repeated and reflection is now obtained for displacements greater than 1.5 cm from the axis of symmetry.

A search for a component of the beam contained in the magnetic field after the beam has been pulsed off has been completed for the symmetric magnet configuration, using a scintillator-photomultiplier combination. The scintillator was placed in the region of the line cusp just beyond the maximum in the magnetic field, and the signal was recorded as a function of time.

In this survey ~ 200 points were recorded, corresponding to crossing a diameter of the vacuum chamber in 1/2 cm intervals for angles of 0°, 5°, 10°, 15°, and 20° to the axis in the plane defined by the axis and the diameter traversed, and for the same angles perpendicular to this plane. In one region (~ 2.5 cm from the axis and inclined 5° perpendicular to the plane of the z-axis and the diameter traversed) the signal exhibited a persistent tail about 100-μsec long. The properties of this tail are as follows:

1) An obstruction placed in the confinement region reduces the tail to zero.

2) The signal disappears if the beam is made short compared to 100 μsec.

3) Biasing the scintillator surface either 300 volts positive or negative has no effect on the signal.

4) The signal is pressure sensitive, and will disappear for pressures below 10^{-6} mm Hg, although it can be comparable to the beam signal at 5×10^{-6} mm.

At the present time it has not been established whether this tail represents an ion beam contained for these times or (a) a perturbation of the gun turnoff time from stray magnetic fields in the accelerating tube, or (b) residual electrons in the containment volume striking the scintillator. Experiments are under way at the present time to determine the origin of this effect.

D. PERHAPSATRON S-5-ZEUS

Measurements of the D-D neutron yield from the Perhapsatron S-5 show marked dependence on the B_z stabilizing field, applied voltage, and deuterium gas pressure similar to that observed earlier with the Perhapsatron S-3 and S-4 machines; the optimum values of B_z and pressure are different for the three machines. The results for PS-5 are summarized in Figs. 5 and 6. A linear rise of neutron yield with voltage is observed (Fig. 5) rather than an exponential increase that would be expected if the plasma temperature increased as the input energy. Two conclusions can be drawn: (a) energy losses dominate and limit any thermonuclear neutron yield, and (b) the effectiveness of runaway or instability processes contributing to the neutron production increases at most linearly with the input voltage.

Measurements of neutron burst shape show that the onset time is ~ 10 μsec after gas breakdown and that this delay is, to a good approximation, independent of voltage and gas pressure. The burst rises rapidly to peak amplitude in ~ 5 μsec and falls off about linearly to give a total burst width of ~ 20 μsec. Larger burst widths up to 40 μsec are observed at operating voltages below 10 kv. The reduction in burst width at higher voltages is possibly correlated with increasing impurity influx observed near peak gas current at the higher voltages.

The impurity radiation (3500 to 8000 A) consists of a strong continuum over the entire spectrum measured, with additional broadened strong line spectra, predominantly from silicon and oxygen. The intensity and onset time of the radiation show marked dependence on voltage and stabilizing field but are insensitive to gas pressure. The onset time occurs in the time interval near peak gas current (~ 30 μsec after breakdown). Some magnetic field probe measurements of the discharge have been made but only preliminary results have been obtained. The discharge starts as a current

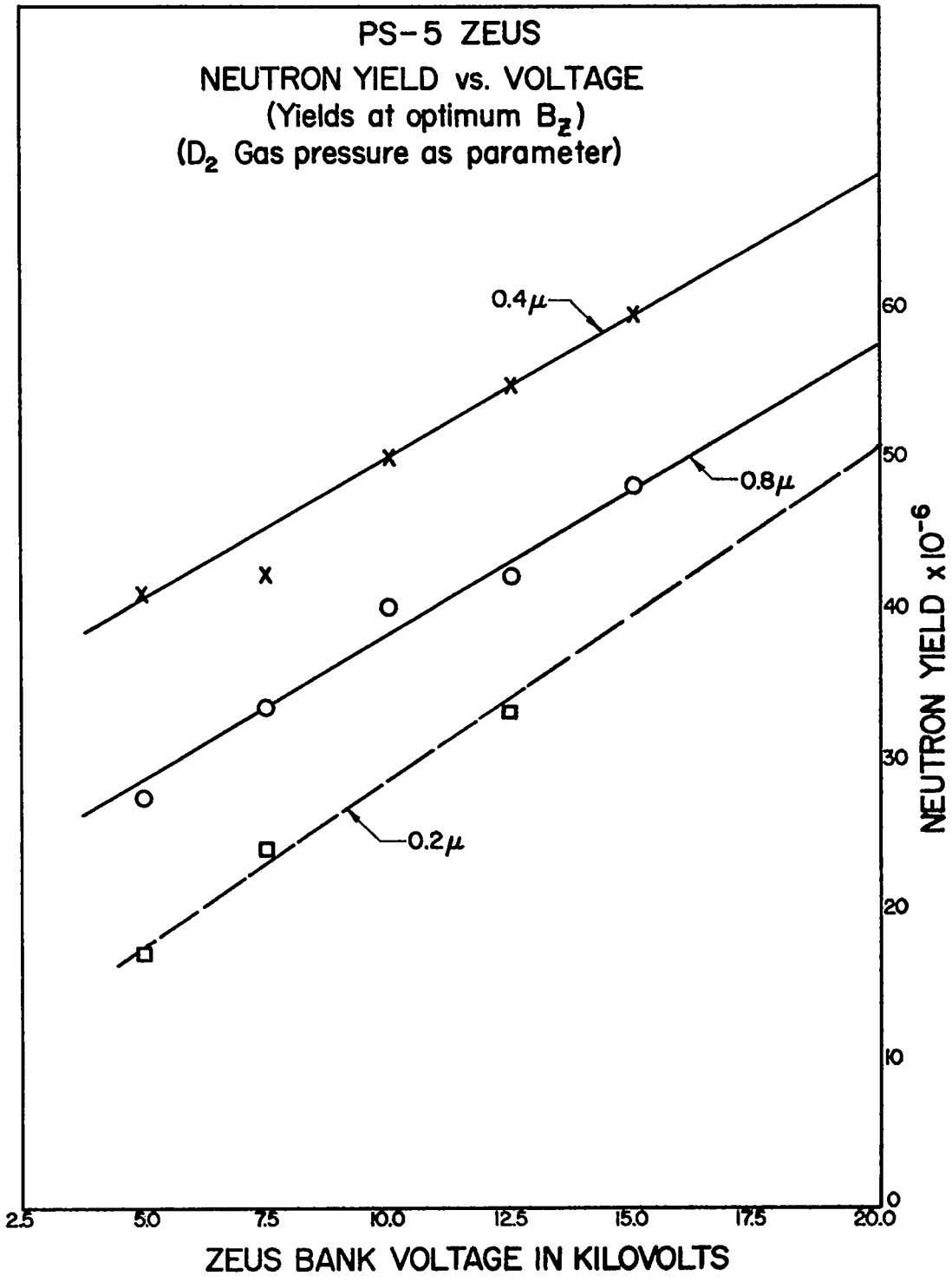

Fig. 5. Neutron yield versus voltage in Perhapsatron S-5-Zeus

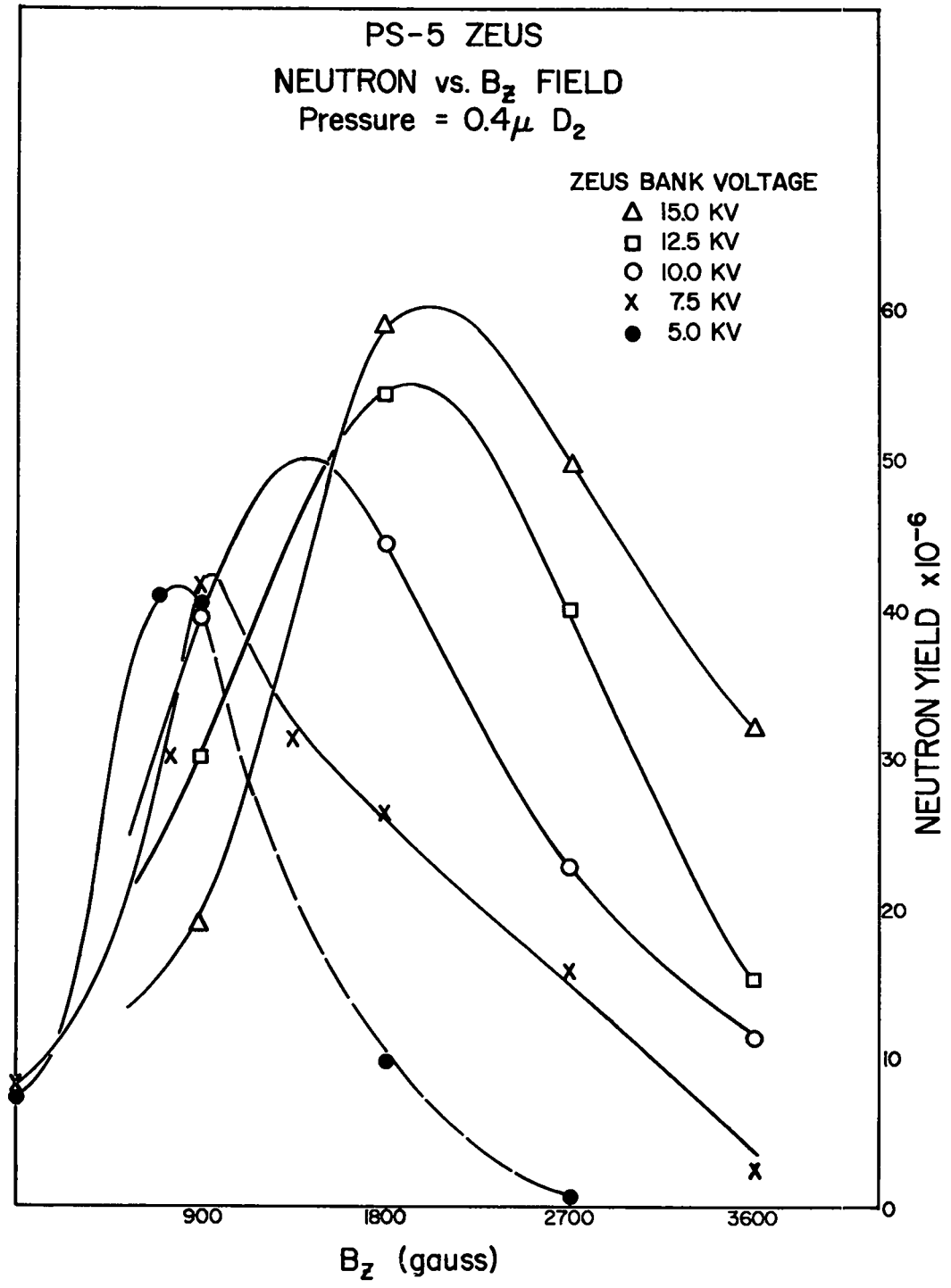

Fig. 6. Neutron yield versus B_z field in Perhapsatron S-5-Zeus

sheath at the torus walls, but the sheath thickens rapidly to a uniform current distribution in ~ 5 μsec. The current channel pinches to ~ 1/2 the torus cross section varying, of course, with stabilizing field and applied voltage. The discharge appears to be grossly stable; however, probe traces obtained at the interior of the plasma are reproducible for only ~ 6 μsec of the discharge period.

E. ORTHOGONAL PINCH

Plasma compression and heating by rising axial magnetic fields (orthogonal pinch) in mirror geometry have been examined using (a) internal and external magnetic probes, (b) streak photographs, and (c) magnetic flux and neutron production as the principal diagnostics.

Recently, Kerr cell photographs (0.1 μsec duration) of the cross section of the discharge were obtained (Fig. 7). At optimum deuterium gas pressures (~ 135 microns), the photographs show a weak diffuse illumination with some irregularities during the second half-cycle time even with the addition of 30% helium to the deuterium. No sharply defined boundaries exist such as had been reported by other experimenters. At pressures of 380 microns (neutron production small) a circular ring structure appears, again not sharply defined, with small perturbations on the inner and outer surface of the ring. These perturbations are not correlated with a wavelength disturbance and do not grow in time. The lack of appreciable light intensity, under optimum operating conditions, was first evidenced by streak photography.

X-ray photographs of the deuterium discharge have been made with the pinhole camera techniques through a thin (225 $\mu g/cm^2$) aluminum-Zapon window. The size of the image indicates a region of hot electrons ($0.1 < T_e < 0.5$ kev) of diameter 1.2 to 2.0 cm.

Two new diagnostic procedures are being developed to obtain a time resolution of the effect of plasma streaming from the mirror geometry. They include the measurement of (a) the $\vec{v} \times \vec{B}$ electric field due to plasma streaming across two electrodes in a crossed magnetic field, and (b) the pressure exerted by the streaming plasma on a piezoelectric crystal.

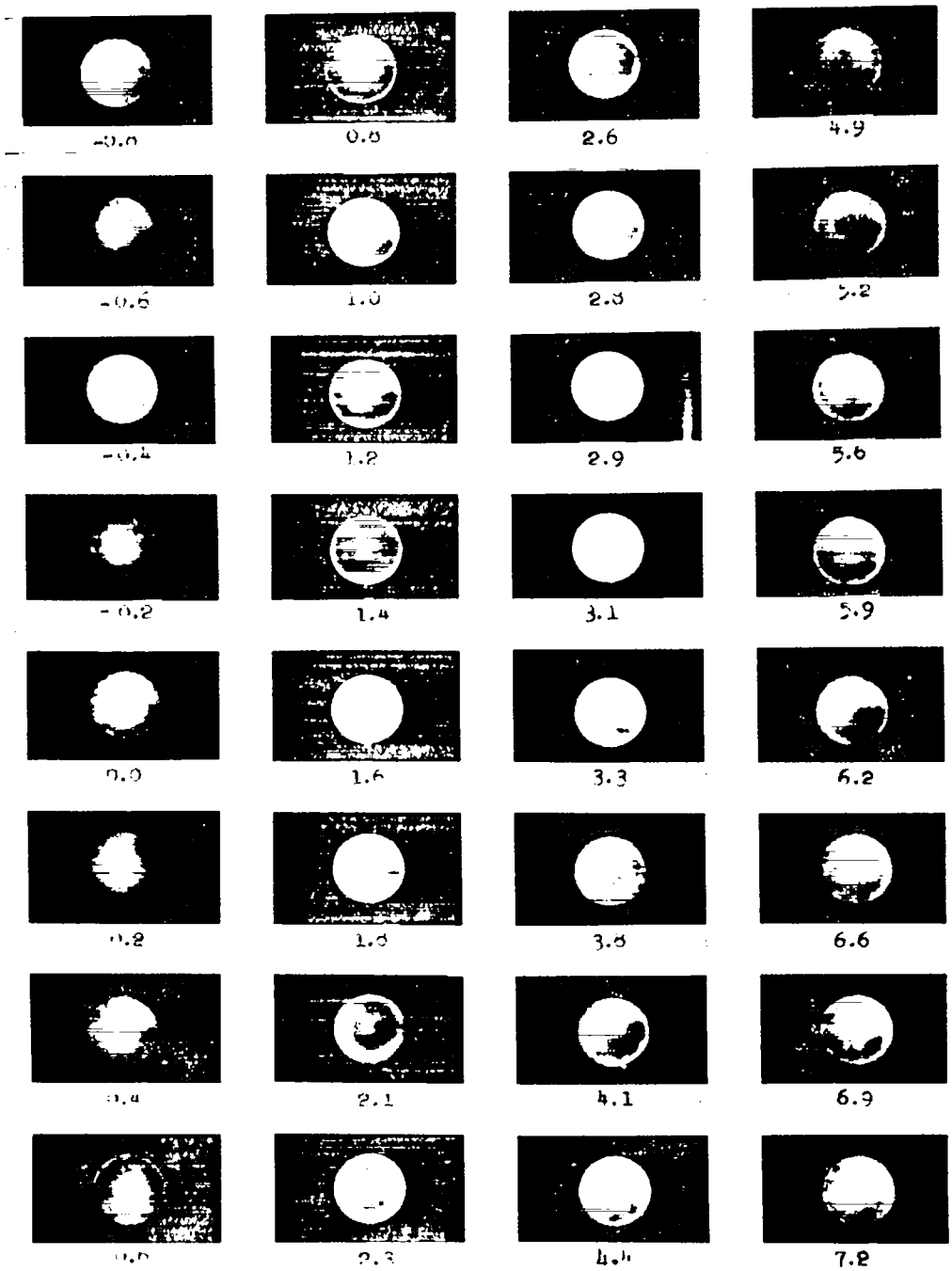

Fig. 7. Kerr cell photographs of a D_2 discharge at 135 microns, V_o 18 kv, diameter 6.6 cm, length 15 cm, R_m = 1.02:1. (Numbers below each photograph are in μsec; 0.0 refers to the start of the second half-compression cycle, 3.3 to the peak field, and 7.2 to the end of the second half-cycle.)

F. SCATTERING OF MICROWAVES BY AN IONIZED GAS

The object of this work, as mentioned in previous reports, is to measure the intensity, frequency spectrum, and angular distribution of microwaves scattered incoherently by the collective electron and ion oscillations in an ionized gas.

Considerable effort has been devoted to increasing the electron density in the scattering chamber, which is a cylindrical Pyrex bottle 1 ft in diameter and 3 ft in height. The major portion of the surface area must transmit microwave power, and cannot be obstructed by rf coils. Experiments were carried out with rf coils (magnetic coupling) and rf straps (electric coupling) attached to the chamber at its extreme ends, using various gases and gas mixtures. The electron density was monitored by a 3-cm microwave interferometer with a limiting sensitivity of $\sim 2 \times 10^8$ electrons/cm^3. At this time an approximately 50-fold increase in electron density has been achieved in a mixture of krypton and mercury, and the maximum density is $\sim 10^{10}$ electrons/cm^3, as measured at two different frequencies. The starting gas pressure varied from 5 to 15 microns, and mercury is always present at about 1 micron. The rf transmitter operates at about 28 Mc (lower frequencies were found to be less efficient) and consists of two Thunderbolt Johnson 1-kw transmitters operating in series and fed by a single driver unit. With this setup frequent transmission line failures are being experienced due to poor voltage standing wave ratio. Attempts to improve the match between transmitters and the plasma are being made.

The radiation pattern produced by the primary power S-band horn has been examined by a receiving horn, with the magnetron operating at 2.6 kMc. The reflection coefficient of the scattering chamber walls has not been measured, but if the published value of the Pyrex dielectric coefficient ($\Sigma \approx 4.0$) is used to correct for reflections, the intensity of the primary beam (at full magnetron power level) inside of the bottle is found to be $\sim 1/40$ watts per cm^2. This is about four times smaller than estimated originally.

The long time stability of the radiometer has been further improved by replacing the dual diode rectifiers in the lock-in detector with a 35-cycle mechanical chopper. In the new arrangement the detector can no longer drift as a result of shifts in the vacuum tube operating conditions. In particular such a detector gives zero output for zero input.

A detailed check has been carried out on the frequency characteristics, in various crystal holders, of 1N21B and 1N369A crystals used to rectify the output of the traveling wave tubes between 3100 and 4100 Mc. The measurements show variations in output level between 1.16 and 2.0 over this frequency range depending upon the choice of crystal. Crystal sensitivities appear to vary by about a factor of 10.

A source of major concern in the work on microwave scattering is the difficulty of satisfying boundary conditions. As previously reported (LAMS-2444, p. 52), what is measured is the Fourier component of the density flucutation, that is, $|\delta n\ (\underset{\sim}{k}_o - \underset{\sim}{k}_\lambda)\ |^2$, where $\underset{\sim}{k}_o$ and $\underset{\sim}{k}_\lambda$ are the wave vectors of the primary and scattered radiation. For 90° scattering, boundary conditions require

$$\frac{n^2}{4D^2} = \frac{2f_o f_p}{c^2} - \frac{f_p^2}{c^2} + \frac{2f_o^2}{c^2} ,$$

where n = 1, 2, 3, ... ; f_o is the primary frequency, and f_p is the plasma frequency. This relationship indicates $n \approx 8$ for the existing working conditions. Uncertainty in this estimate is associated with the density gradients in the scattering chamber. Experimentally it may be difficult to adjust all of the experimental parameters to satisfy boundary conditions. If this is so, a shift to higher primary frequencies is indicated.

G. IXION

General

Experiments have been performed to determine (a) the degree of ionization of the Ixion plasma, (b) the amount of energy loss to the wall, and (c) the nature of the particles carrying away the energy. The conclusion is that at least a major portion of the plasma is fully ionized and that most of the energy loss of the machine, that gives rise to the voltage limiting effect, is accounted for by hard ultraviolet radiation from impurities.

Results of Ultraviolet Spectrum Analysis

The Jarrell Ash (Seya-Namioka) vacuum monochromater was used to examine the spectrum from the Ixion plasma at its midplane. Among many prominent lines lying between 400 A and 4000 A, positive identification was made of the C IV doublet at 1548 A and the corresponding N V and O VI doublets at 1238A and 1032A. The O VI line became less intense as the machine cleaned up with discharges. The N V line was observed only when nitrogen was introduced as a contaminant in the injected gas. It is clear, therefore, that an appreciable portion of the plasma is fully ionized. According to the corona equation the presence of O VI implies an electron temperature of 18 ev or greater.

Bolometer Measurements of Energy Loss to the Wall

The energy flux to the wall at the Ixion midplane was measured absolutely in a time-resolved manner by observing the temperature rise of a thin metal disc. The geometry of the experiment is shown in Fig. 8. A carbon-blackened, 0.3-mil, molybdenum foil target was positioned near the wall in a glass tube so as to intercept a portion of the escaping energy. Its temperature rise during the discharge was then measured as a function of time by means of an infrared detector. The instrument was calibrated absolutely by duplicating the geometry, and measuring the detector output voltage when focussed on a molybdenum target heated to a

GEOMETRY FOR INFRARED DETECTOR

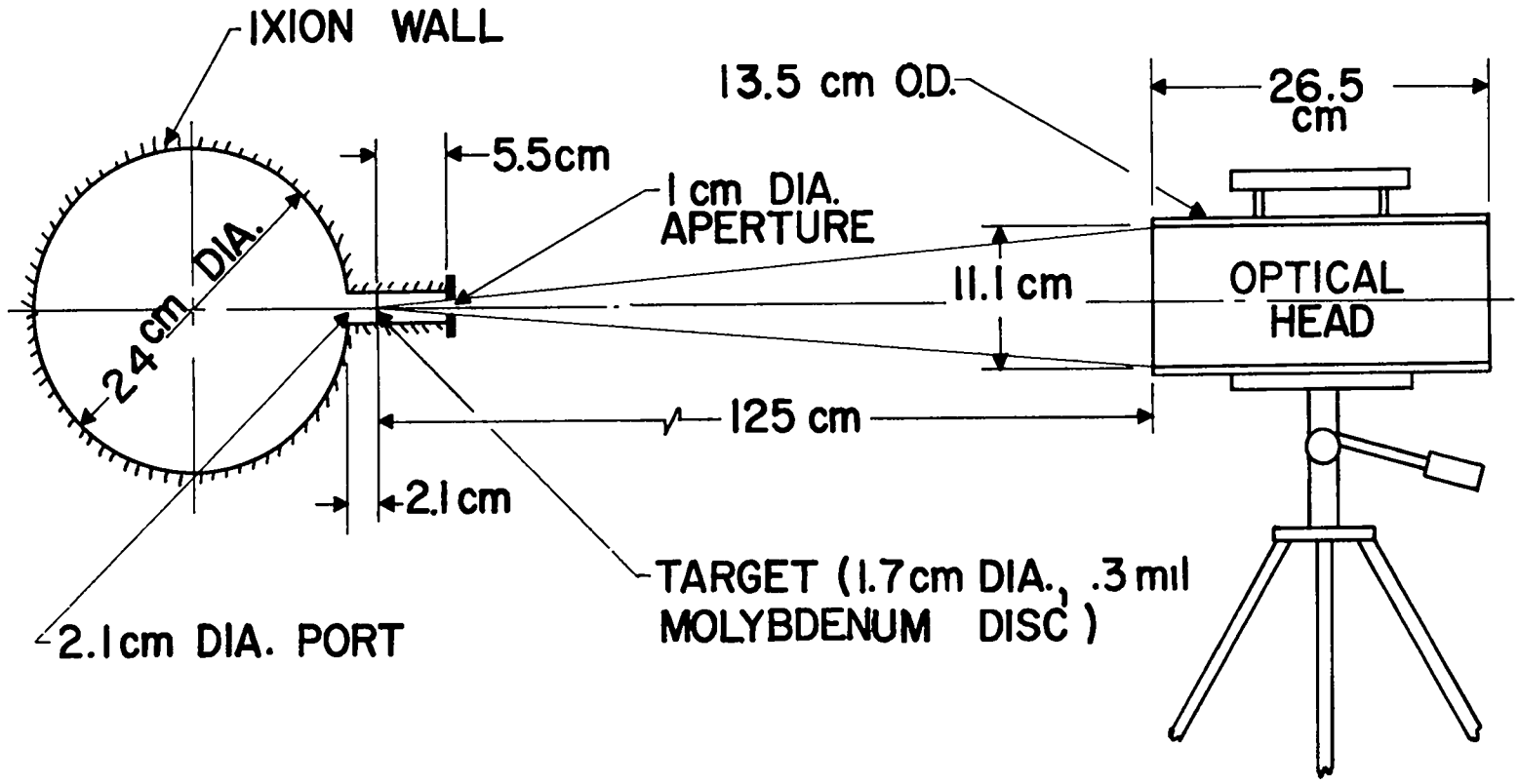

Fig. 8. Geometry of bolometer measurement of energy loss in Ixion

known temperature. The data from Ixion were taken through a sapphire window and calibration curves were obtained for sapphire and calcium fluoride windows as well as with no window. For normal operation (V_o = 7.5 kv, B_o = 8.2 kgauss) the total energy deposited on the molybdenum foil is

$$W(\text{normal}) = 0.9 \text{ joules}.$$

For boosted operation (V_o = 7.0 kv, V_{boost} = 10 kv, B_o = 8.2 kgauss),

$$W(\text{boosted}) = 1.4 \text{ joules}.$$

Taking into account the area of the molybdenum disc and making an approximate solid angle correction, the energy densities detected at the Ixion wall after the unboosted and boosted discharges are 1.6 and 2.8 joules/cm^2, respectively.

The temperature rise of the molybdenum disc and the power and energy input from the capacitors to Ixion are plotted as functions of time in Figs. 9 and 10. It will be noted that, except for a constant scale factor, the temperature rise and energy input curves are almost the same. This indicates that the power loss of Ixion is accounted for by the external radiation as seen on the bolometer. The scale factor is evaluated below from a consideration of the plasma geometry in order to compare the absolute energy input with the energy radiated.

Since lithium fluoride transmits in the ultraviolet about 1200 A, a LiF window was placed over the disc in order to determine the portion of radiated energy carried by long wavelength photons. A small signal of only a few percent of that observed without the window was detected. This means that radiation above 1200 A cannot account for more than a small proportion of the energy flux to the Ixion wall. After a few discharges the signal through the window disappeared, probably due to the formation of a coating on the LiF window.

Pinhole Photograph with SWR Film

A pinhole photograph of the Ixion discharge was also made, for the purpose of determining the density of energy carried to the walls by

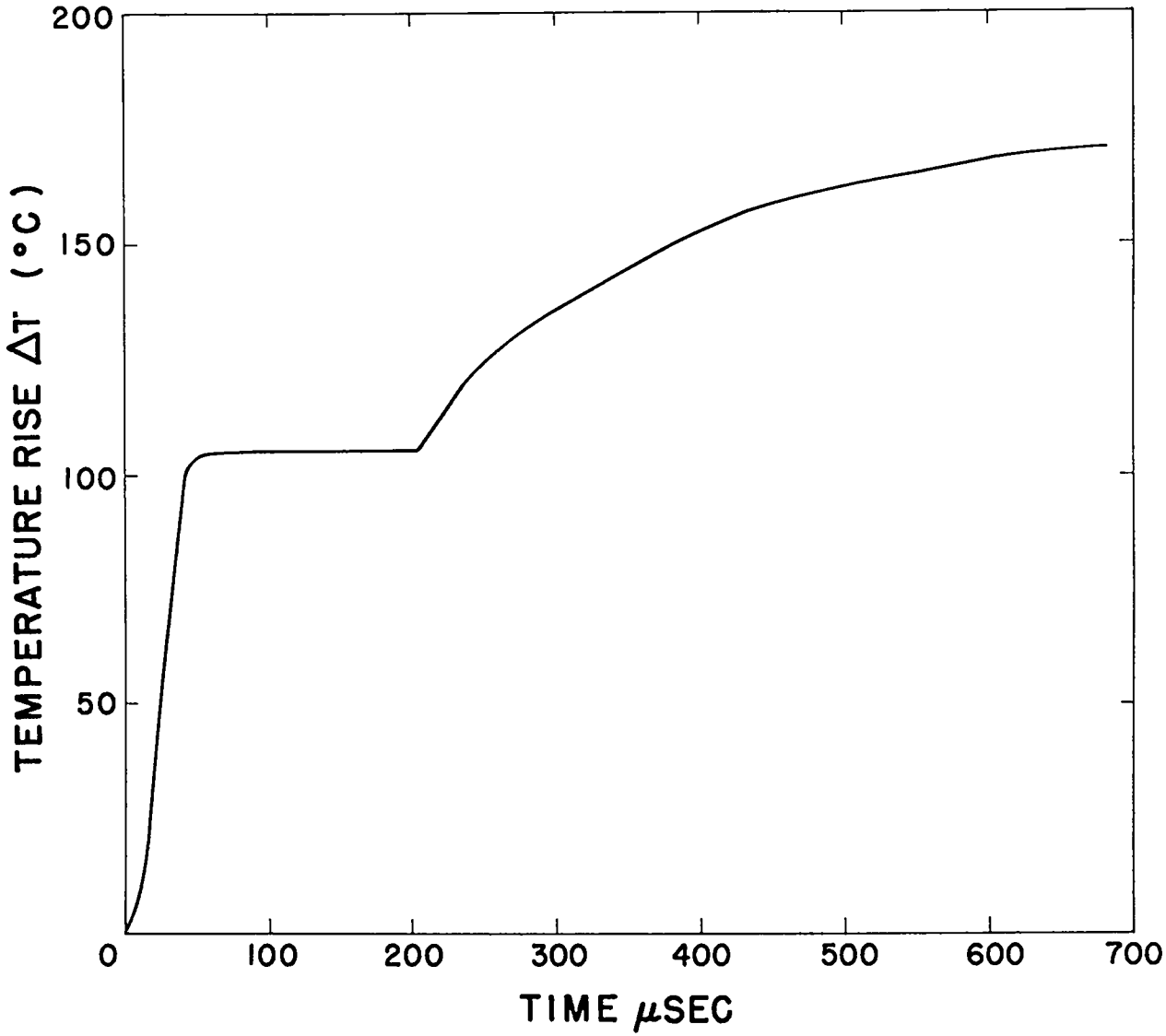

Fig. 9. Temperature rise of molybdenum disc and power and energy input versus time

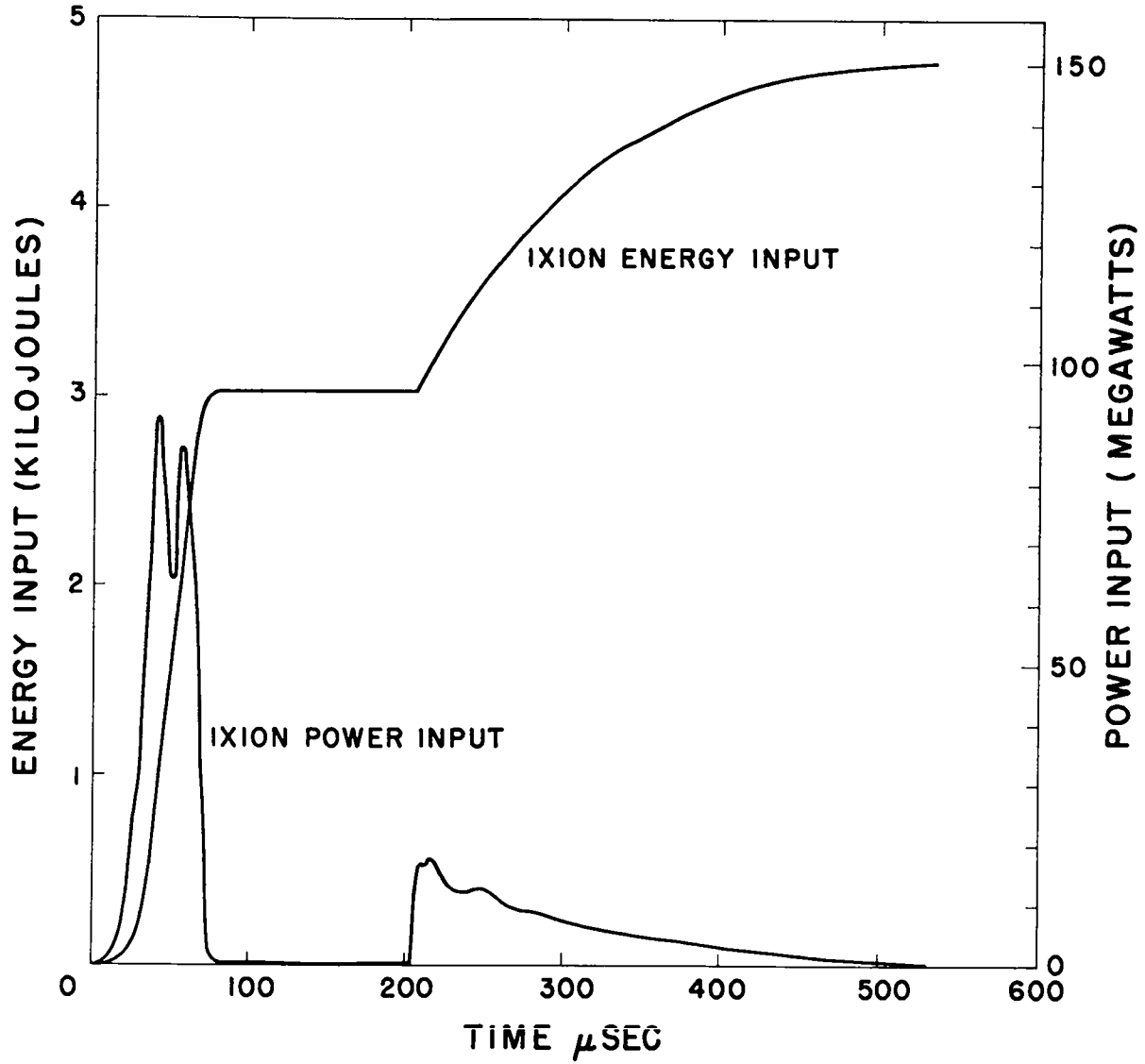

Fig. 10. Ixion energy and power input versus time

photons. The real difficulty in the method arises from the fact that no experimental sensitivity data are available between the soft x-ray region and 1216A. From the available information, a sensitivity in this far ultraviolet region of from 1/2 to 1 times that at 1216 A is predicted.

The sample of SWR film was calibrated by comparison with the known sensitivity of a standard film at 4000 A. The result of exposure to one shot (unboosted) gave a density of 10 ergs/cm^2 at the wall. This agrees reasonably well with the bolometer figure. The presence of the 8.5 kgauss field prohibits any deuteron under 100-ev energy from reaching the film.

Photo-Cell Measurements

The fourth detector used to look at the radiation from Ixion was a palladium photo-cell. The presence of the magnetic field and the small angular acceptance served to eliminate all charged particle effects. The power into Ixion (V.I) and the photo-cell current are shown as a function of time in Fig. 11. The photo-cell current follows the power but with an apparent time delay of 5 to 10 μsec. This delay may be associated with time for populating the higher ionized states of the contaminants.

When the total integrated photo-cell current is compared with the energy measured at the wall, with both the foil and the ultraviolet camera, an average photon energy of 60 to 100 ev is indicated. Such photon energies would be expected from the highly ionized contaminants whose longer wavelength lines were observed in the discharge. Therefore it is concluded that a major portion of the energy loss in Ixion and the attendant voltage limitation are accounted for by electromagnetic radiation from these contaminants.

Conclusion

The results from both the energy density measurements should be compared with the density expected at the wall assuming Ixion to be radiating all of its energy in the ultraviolet. Defining the radiating volume by earlier probe measurements, the normal (unboosted) Ixion input of $\sim$ 3000 joules gives a density of 1.7 joules/cm^2 at the wall. Thus, within the accuracy of these measurements the radiation detectors at the wall account for all of the energy input to Ixion.

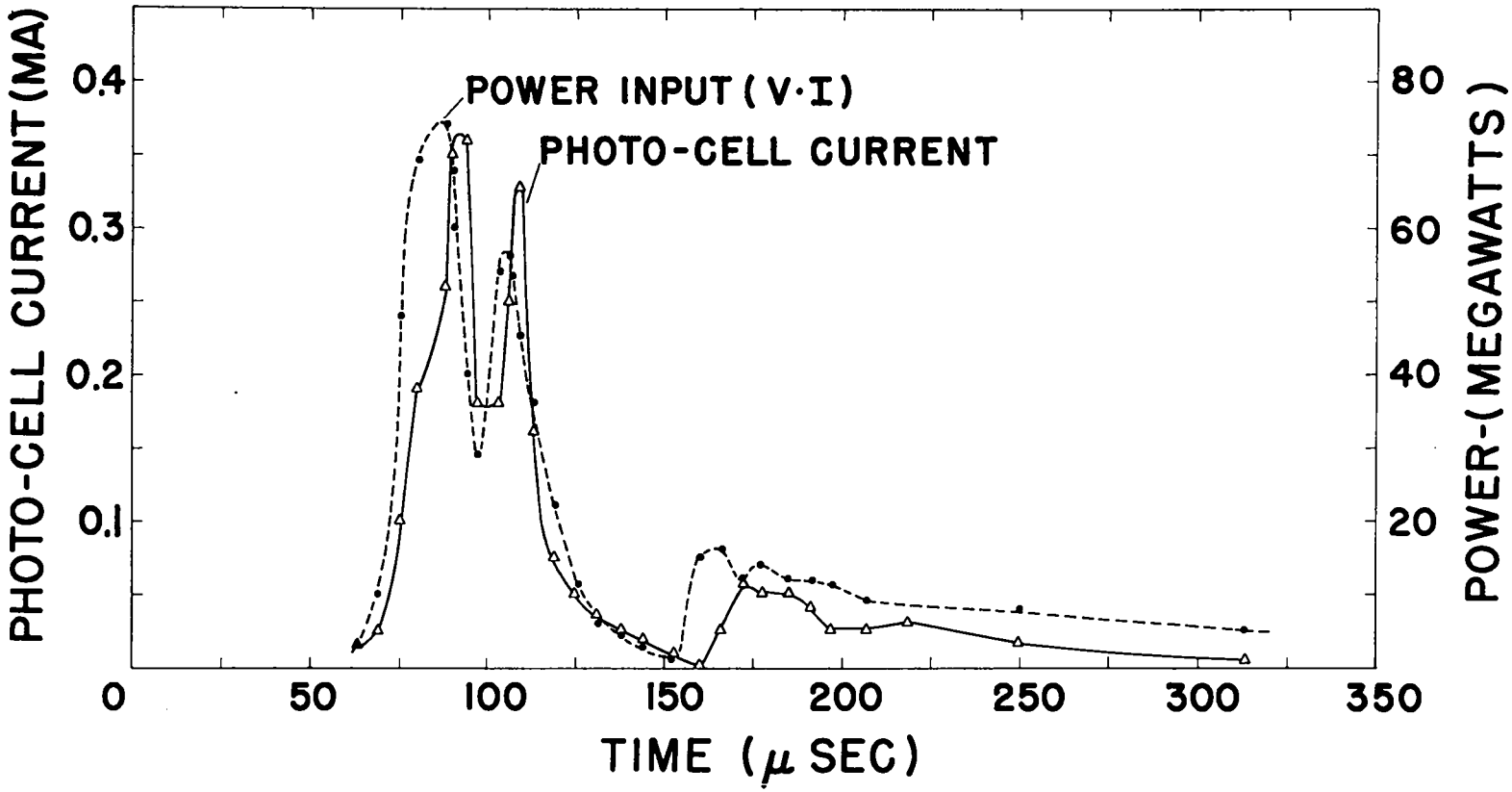

Fig. 11. Power and photo-cell current into Ixion as a function of time

E X B Gun

The old Ixion experiment has been dismantled, and a new, linear, $\vec{E} \times \vec{B}$ experiment is being started. Its object is to accelerate plasma adiabatically by means of the $\vec{j} \times \vec{B}$ force arising from:

1) The plasma displacement current which is drawn when the drift velocity (E/B) along the gun increases.

2) An externally impressed magnetic field which decreases in magnitude along the gun.

The electric field is to be constant, and the external magnetic field will be modified by the displacement current.

The apparatus is to consist of a Marshall gun which injects plasma at the breech of the $\vec{E} \times \vec{B}$ gun. The latter consists of a pair of long rectangular coils to furnish a magnetic field between the plates, parallel to their surfaces.

The Marshall gun was designed as a clean system with copper gaskets and ceramic-metal seals and has been installed on a clean, bakable vacuum system. The rectangular coils have been constructed and are being installed. Construction is under way on the capacitor system for driving the Marshall gun. It consists of two G.E. Clamshell capacitors with special low-inductance adaptors for the ignitron switches. The coils will be energized by the same 3-kv bank which was used on the Ixion coil. In addition, most of the control circuitry from the old experiment has been taken over.

H. SCYLLA

Soft X-Ray Measurements

The soft x-ray spectrometer (LAMS-2464, p. 17) has been used successfully to diffract radiation from the Scylla I plasma. Since the plasma provides an extended source, collimation is provided by means of identical Soller slits on the source and detector arms. The angular resolution of each slit is $\pm$ 11 min.

Two preliminary experiments have been performed. The Scylla discharge was first loaded with 6% neon in order that the helium-like triplet and singlet series of the impurity could be observed, as well as the hydrogen-like Lyman series. (The helium-like series of the normal oxygen impurity occurs at wavelengths too great to be diffracted by the beryl crystal). The results, uncorrected for crystal reflectivity, are shown in Fig. 12. The occurrence should be noted of both singlet and triplet lines of Ne IX with almost equal intensities, as predicted by Edlen on the basis of the breakdown of LS coupling at high Z values. The strong line at 13.66A is possibly $1s^2 1s_o - 1s^2 s^3S_1$; a corresponding line in adjacent elements has been reported in the literature. In addition to these lines, several nondiagram satellites are seen which are probably screened transitions in the 3-electron Ne VIII system, such as $1s^2 2s - 1s - 2p^2S$. The identification is based on the time history of the discharge, which shows the satellite lines to occur before Ne IX lines, as is to be expected for transitions arising from less completely ionized ionic species.

The first two Lyman lines of Ne X are observed, and their time history shows them to occur later during the magnetic compression than the Ne IX lines, as is expected

The Scylla discharge was also loaded with 10% oxygen in order to increase the intensity of the spectral lines over that of the continuum. Five Lyman lines are seen (see Fig. 13) beginning with L_γ. The lines L_α and L_β lie outside the range of the spectrometer. Measurements with no added contaminant also show prominent O VIII Lyman lines, but with a smaller

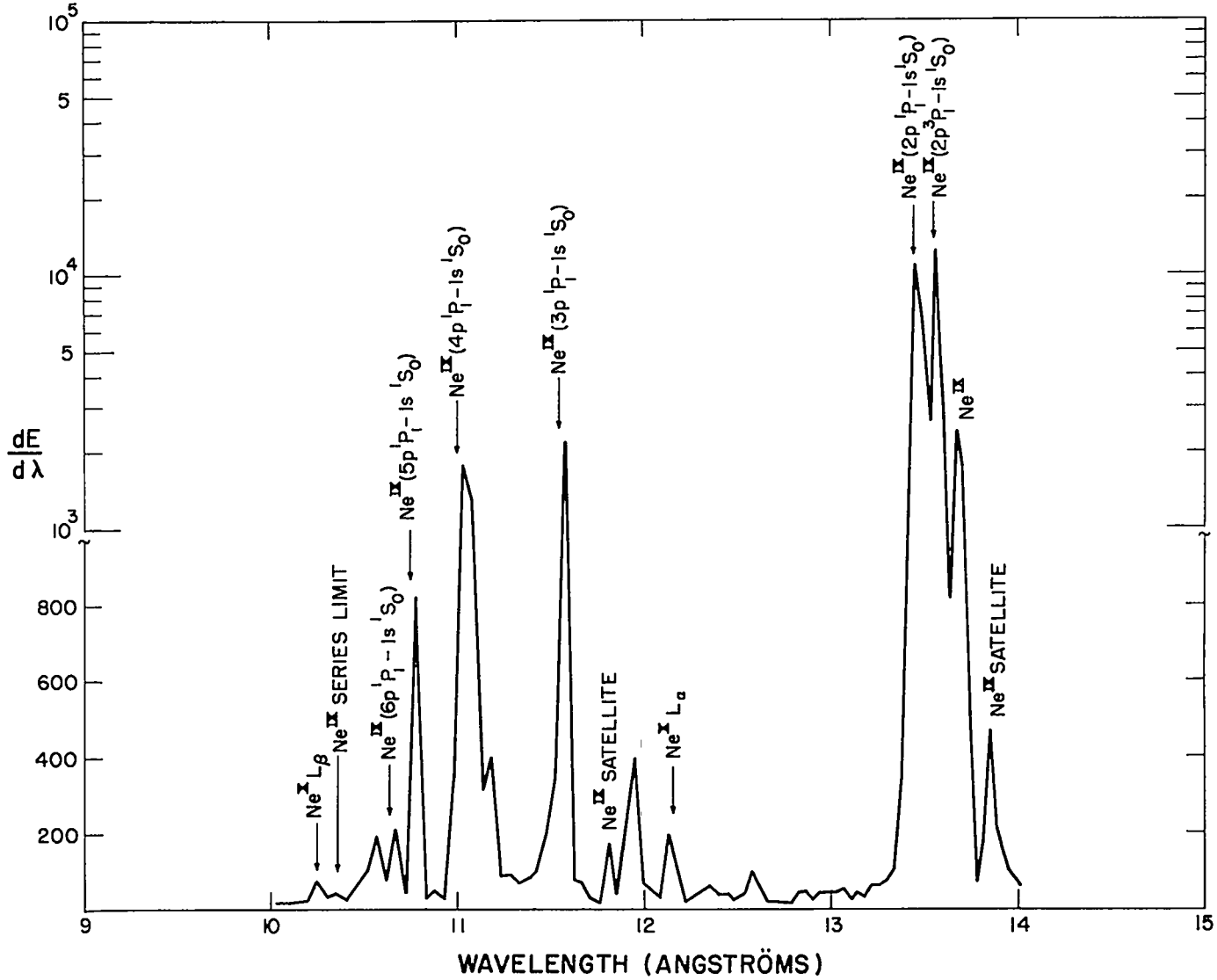

Fig. 12. Soft x-ray spectra from Scylla discharge with 6 percent neon.

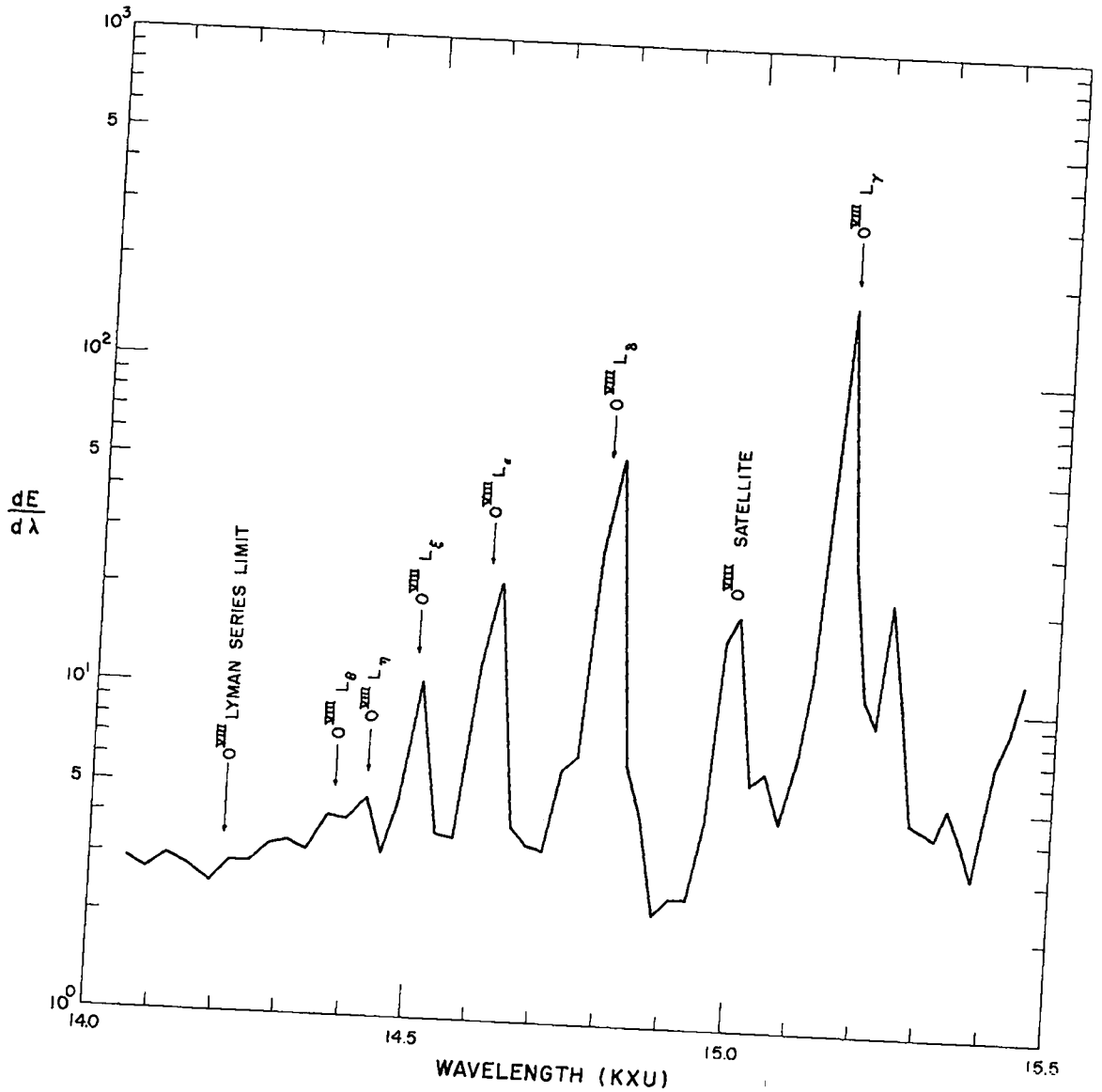

Fig. 13. Soft x-ray spectrum from Scylla discharge with 10 percent oxygen.

ratio of line intensity to continuum intensity. In no case is an appreciable discontinuity of the continuum intensity observed at the series limit of an ionic species.

Measurements are proceeding to measure the reflectivity of the crystal as a function of wavelength, using various characteristic lines generated in an x-ray tube.

Scylla III

The assembly of Scylla III has been completed, except for installation of the power crowbar capacitor bank. After 43 discharges, two of the forward sections of the parallel plate transmission lines were modified to improve the crowbar gap section. The control and signal wiring was completely redone, using new cable ducts, in order to reduce electrical pickup to a sufficiently low level for taking data.

The machine has been run on the second half-cycle with the main bank charged to voltages of from 70 to 85 kv, using two coils:

1) A coil having the same dimensions as the normal Scylla I coil (length 10.6 cm, inductance 0.038 μh).

2) A coil of 18 cm length with an inductance of 0.024 μh which is otherwise the same as the first coil.

So far only current, voltage, and neutron yield have been measured. Neutron yields as great as 5×10^7 occur, indicating that the plasma temperature has increased appreciably over that of Scylla I. The rise time of the magnetic field with the first coil is now 2.0 μsec and the maximum amplitude used so far is 120 kgauss.

A B_z-type preionizer is being designed, based on Axel Brothers 50 kv, 1 μf capacitors, to couple directly to the compression coil and to withstand the 120 kv which will be applied to it from the main capacitor bank.

I. ZEUS

Installation of the first half of the Zeus capacitor bank has been essentially completed. The basic construction of the bank is shown in Fig. 14 which is a photograph taken during construction. The present arrangement with two experimental areas adjacent to the bank is shown in Fig. 15. The left hand area contains the Perhapsatron S-5 experiment while the right hand area is set up for bank testing.

Preparations are underway for testing the 32 newly completed sections of the bank. Such tests consist of firing each tier (or section) into a dummy load for 100 discharges at 20 kv and 500,000 amp. The inductance of the system, (shelf, cables, and load) is such that the ringing period is 170 μsec with 85% voltage reversal. Experience has shown that such tests are adequate to eliminate weak capacitors and to test out the firing and transmission systems.

The test load for this work consists of a 36-in. wide sheet of 1/4 in. aluminum rolled into a 45-in. diameter circle. The load and its cable connections are shown in Fig. 16. Such a design, although somewhat bulky, has proven to be a very stable load for the currents involved.

Components have been received and assembly work is proceeding to convert one tier of the bank to a faster (low inductance) transmission system. Calculations indicate that with the use of special low-inductance cable the shelf inductance will be reduced to 0.028 μh. This will give an inductance per megajoule of 0.004 μh, and will bring the Zeus system into an inductance range which is of considerable interest for fast experiments.

Fig. 14. Zeus capacitor bank during construction.

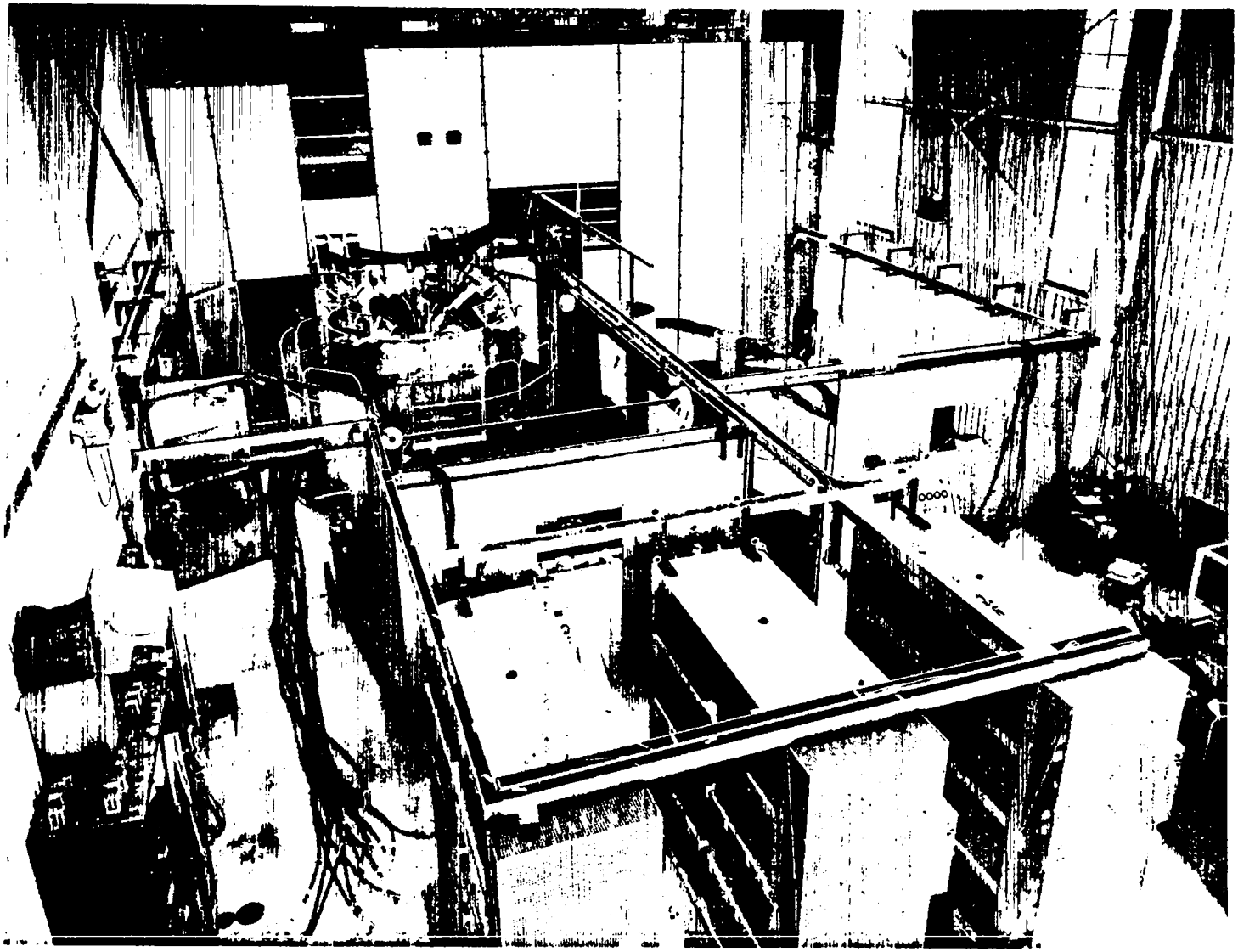

Fig. 15. Arrangement of Zeus experimental areas, showing Perhapsatron S-5

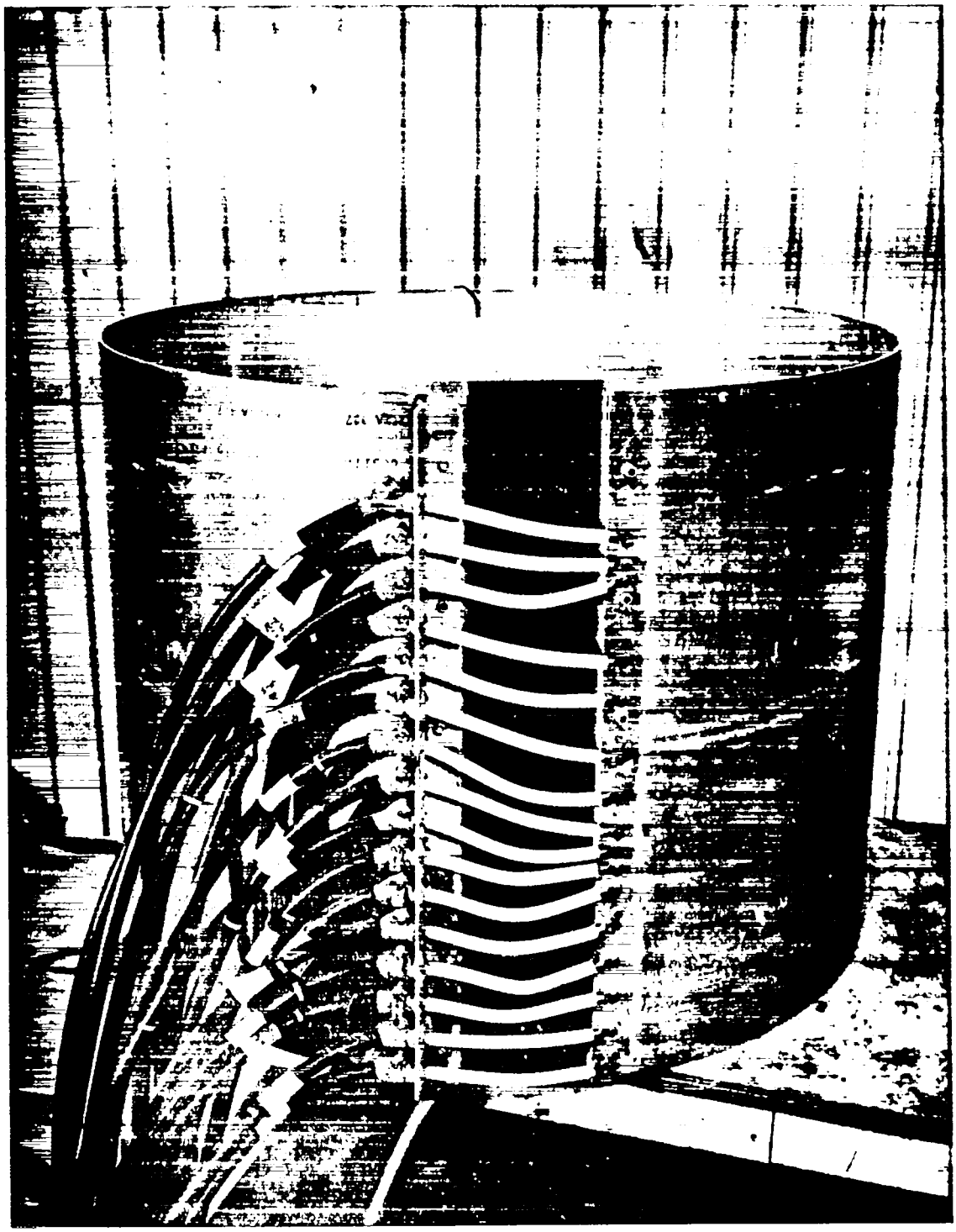

Fig. 16. Load and cable connection for testing capacitors.

J. COMPONENT DEVELOPMENT

High-Voltage Test Facility

Installation of the test banks and charging supplies has progressed. One bank is now in use evaluating capacitors from various manufacturers for replacements in Zeus. Life tests can be run automatically at a rate of about 500 discharges per day. In addition, facilities are nearing completion for testing ignitrons, spark gaps, and special high-voltage circuits.

Capacitor Development

In order to determine the relative merits of the various energy storage capacitors now available, a program was undertaken to measure the capacity, Q value, and ringing frequency of all the units now in use at Los Alamos. In addition, small numbers of several new types of capacitors have been purchased for test and evaluation. The results of these measurements are given in the accompanying table. The resonant frequency figures are averages of the values obtained from several units of each type. They are considered as nominal values and provide a relatively good comparison. In a few cases extreme efforts were used to minimize the external inductance and these values are indicated.

In actual practice these figures are somewhat academic since the capacitor must be connected to a header or transmission system. However, they do give an indication of the relative comparison between units.

Development work has been proceeding on a fast parallel plate capacitor. Two prototype units have been fabricated with characteristics as follows:

1) Circular capacitor with coaxial header

   $C = 0.55\ \mu f$ $\qquad$ $L = 0.009\ \mu f$

   $f_r = 2.24$ Mc $\qquad$ $Q = 33$ at 2.25 Mc

2) Rectangular parallel plate capacitor

   $C = 0.44\ \mu f$ $\qquad$ $L < 10^{-9}$

   $f_r = 9.7$ Mc $\qquad$ Q

Electrical Characteristics of Energy Storage Capacitors
in Use by the Los Alamos Sherwood Group

V(kv)	C(μf)	Mfr	Type	f_r(kc)(1)	L(μh)(3)	Q
3	100	Aerovox	PX21J5	91.8	0.03	10 (40 kc)
20	7.65	G.E.	14F645	238	0.058	14.1(120 kc)
20	14.4	G.E.	14F745	201	0.043	15.4(78 kc)
20	14.7	Tobe	XN273	202(2)	0.042	12.8(78 kc)
25	0.475	Bosch	K03GH357	1450	0.025	11.1(1 Mc)
40	0.1	Tobe	NRG341	4120	0.014	16 (1 Mc)
50	1.08	Axel	50E104	1450	0.011	15.5(500 kc)
50	1.02	G.E.	14F680	1380	0.013	13.4(500 kc)
50	0.93	G.E.	14F756	1400	0.014	11.2(616 kc)
50	1.0	Tobe	XN250A	776	-	13.8 (776 kc)
100	0.5	BICC	X1189	460	-	-
100	0.8	Tobe	XN249	542	0.101	42.5(100 kc)
120	0.65	C-D	XN249KR	612	0.105	19.4(100 kc)
120	0.8	Tobe	XN249K	630(4)	-	

Notes:

1. Resonant frequency quoted is the driven resonant frequency with a minimum inductance external strap configuration.

2. A special close fitting spark gap assembly gave a ringing discharge frequency of 211 kc at 5 kv on a 14.7 μf Tobe, giving an estimated inductance of 0.039 for the capacitor.

3. Inductance values are not necessarily minimum values but are obtained using a standard low-inductance shorting strap for comparative evaluation.

4. Resonant frequency measured with a copper can surrounding the insulator to contain the field in addition to a close strap assembly. The configuration approximates a tight coaxial system.

These units have been constructed with Mylar as the dielectric. Although Durathene would be a preferable material for a number of reasons, a method has not been found as yet for bonding it to the copper plates. Difficulties have also been encountered with the header design on these units so that at present they are rated at only 20 kv. Modifications to the header and the basic construction are being made to bring the unit to a 50 kv ringing rating. Further tests are underway to evaluate the design under discharge service. When a suitable design is found, a 0.5 μf, 50 kv unit will be built in a complete package with a header for connecting it to a parallel plate transmission line.

Ignitrons

Calculations and measurements have been made on the GL7703 (Z5385) ignitron which was developed through the joint effort of LASL and the General Electric Company and which is now widely in use througout the Los Alamos Sherwood group. In making such calculations, assumptions had to be made concerning where the current flows in the tube in relation to the external return path. Several different calculations were made which agreed in general to about 10%.

A high current ringing measurement was made using three different ignitron header configurations. By determining the resonant frequency of the capacitor and header alone, and with one, two, and four ignitrons, a value for the inductance of the ignitron was determined to be 0.02 μh. This value appears to be relatively constant with currents above 25 ka. Below 25 ka the inductance is slightly higher.

K. PUBLICATIONS

Papers entitled as follows have been submitted for publication to The Physics of Fluids:

"Effects of Ionization and Magnetic Initial Conditions on a Magnetically Compressed Plasma (Scylla)," by E. M. Little, W. E. Quinn, and F. L. Ribe.

"Self-Consistent Reversed Field Sheath," by R. C. Mjolsness, F. L. Ribe, and W. B. Riesenfeld.